Journal of Molecular Catalysis, 84 (1993) 193-205
Elsevier Science Publishers B.V., Amsterdam

M203

Characterization of CrO_3/Al_2O_3 catalysts under ambient conditions: influence of coverage and calcination temperature

Michael A. Vuurman [1], Franklin D. Hardcastle [2] and Israel E. Wachs*

Zettlemoyer Center for Surface Studies and Department of Chemical Engineering, Lehigh University, Bethlehem, PA 18015 (USA); tel.(+1-215)7584274, fax.(+1-215)7583079

(Received June 9, 1992; accepted June 1, 1993)

Abstract

The CrO_3/Al_2O_3 catalyst system was investigated by Raman spectroscopy, X-ray photoelectron spectroscopy, X-ray diffraction, and BET surface area measurements in order to determine the molecular structures and monolayer coverage of the surface chromium oxide phase under ambient conditions. Up to a surface coverage of 9% CrO_3/Al_2O_3, the chromium oxide is stabilized by the alumina support in the +6 oxidation state after calcination at 120-1050°C. The molecular structures of the chromium(VI) oxide surface species are a function of the surface coverage and calcination temperature because under ambient conditions the surface structures depend on the net surface pH at point of zero charge of the hydrated oxide surface. Increasing the surface coverage results in a decrease of the net surface pH and formation of more polymerized chromium oxide species. High calcination temperatures ($\geqslant$950°C) cause a reduction of the BET surface area, as well as a phase transformation of γ-Al_2O_3 into θ,δ-Al_2O_3, and also result in an increase in the surface density of the chromium oxide overlayer (more polymerized surface chromium oxide species). Monolayer coverage is reached at *ca.* 12% CrO_3/Al_2O_3 and crystalline Cr_2O_3 particles are found on the alumina surface together with surface chromium oxide species at higher loadings. At high calcination temperatures ($\geqslant$800°C), the Cr_2O_3 crystalline particles react with the alumina support to form Cr(III) in solid solution with α-Al_2O_3 (corundum). The α-Al_2O_3 lattice is slightly expanded due to the incorporation of chromia.

Key words: aluminium; calcination temperature; chromium; coverage

Introduction

Supported chromium oxides are well known to possess high catalytic activity in hydrogenation and dehydrogenation reactions of hydrocarbons, dehydrocyclization of paraffins, and polymerization of olefins [1]. It is now generally accepted that the catalytic properties of these systems are due to surface

*Corresponding author.

[1]On leave from: Anorganisch Chemisch Laboratorium, Universiteit van Amsterdam, Nieuwe Achtergracht 166, 1018 WV Amsterdam, Netherlands.

[2]Present address: Sandia National Laboratories, Div. 1845, Albuquerque, NM 87185, USA.

chromium oxide species and not to bulk chromium oxide phases such as crystalline CrO_3 or Cr_2O_3 [2]. This knowledge has led to much interest in the molecular structures of the surface chromium oxide phases and in the factors which determine these chromium oxide surface structures [2–21]. A program has been started to study the supported chromium oxide system as a function of surface coverage, support type, calcination temperature, and presence of moisture [19–21]. For the CrO_3/Al_2O_3 system, it was shown that after impregnation with CrO_3 solutions and drying at 25°C under vacuum, the chromium oxide is present as hydrated chromate species at 2% CrO_3/Al_2O_3, as hydrated dichromate species between 10 and 30% CrO_3/Al_2O_3, as hydrated trichromate species at 40% CrO_3/Al_2O_3, and as crystalline CrO_3 and hydrated trichromate species at 60% CrO_3/Al_2O_3 [19]. After calcination at 500°C and re-exposure to the laboratory atmosphere (ambient conditions), it was found that in the 0.5–5% CrO_3 loading range, chromium oxide is present as hydrated chromate and dichromate species and that the ratio monomers/dimers decreases with increasing surface coverage [20]. *In situ* dehydration of these CrO_3/Al_2O_3 samples causes the transformation of the hydrated chromate and dichromate species into two dehydrated species, each possessing one short terminal Cr=O bond, and one or more polymeric species [21]. The dehydrated surface structure was found to be independent of surface coverage in the 0.5–9% CrO_3 range.

In the present paper, the influence of loading (5–24% CrO_3/Al_2O_3) and calcination temperature (120–1050°C) on the surface chromium oxide structures are studied under ambient conditions by Raman spectroscopy. Furthermore, X-ray photoelectron spectroscopy (XPS), X-ray diffraction analysis (XRD), pH at point of zero charge measurements, and BET measurements are used to gain additional information on the chromium oxidation state, chromium oxide and alumina phases, surface acidity, and surface areas, respectively.

Experimental

Sample preparation

The supported chromium oxide catalysts were prepared by the incipient-wetness impregnation of γ-Al_2O_3 (Harshaw, 180 m^2/g) with an aqueous solution of chromium nitrate, $Cr(NO_3)_3$. After the impregnation step, the samples were dried at room temperature overnight, followed by additional drying at 120°C overnight. Finally, the CrO_3/Al_2O_3 samples were calcined at temperatures ranging from 250°C to 1050°C for 16 h. The surface coverages are expressed as wt% of CrO_3.

Raman studies

The Raman apparatus consisted of a Triplemate spectrometer (Spex, Model 1877) coupled to an optical multichannel analyzer (Princeton Applied

Research, Model 1463) equipped with an intensified photodiode array detector (1024 pixels, cooled to −30°C, resolution 1 cm^{-1}). The Raman spectra were recorded approximately 1 h after the calcination step. The samples were pressed onto KBr and spun at 2000 rpm to avoid local heating effects as much as possible. The acquisition time per scan was 30 s and 10 scans were averaged. The 514.5 nm line of an Argon ion laser (Spectra Physics) was used as the excitation source. The laser power at the sample was 1–100 mW.

XPS measurements

The XPS spectra were obtained on a Leybold–Heraeus LHS-10 electron spectrometer. The X-ray source was obtained from an aluminium anode operating at 12 kV and 25 mA, and the binding energies of the Cr $2p_{3/2}$ signals were referenced to the Al 2p peak at 74.5 eV. The XPS measurements were performed at 5×10^{-9} Torr.

X-ray diffraction

The identification of the crystalline phases was performed on a Philips diffractometer using Cu K_α radiation and a diffracted beam monochromator. Lattice parameters were determined with the Least Square Unit Cell Refinement Program of the Material Research Laboratory of the Pennsylvania State University.

BET surface area measurements

The BET surface areas were obtained with a Quantsorb surface area analyzer (Quantachrome corporation, Model OS-9) using nitrogen gas.

Point of zero surface charge (PZC) measurements

The PZC of Al_2O_3, and CrO_3/Al_2O_3 samples were determined by the mass titration method. A 0.1 M NaCl solution was prepared using distilled, deionized, and degassed water. Various amounts of solid samples were added to Erlenmeyer flasks and sealed. The flasks were evacuated and backfilled with nitrogen. The NaCl solution was transferred to the flasks under a nitrogen atmosphere. The oxide/water solutions were stirred overnight. The pH of each solution was measured after 24 h of stirring. The pH meter was calibrated before each measurement.

Results and discussion

Influence of surface coverage

In a previous investigation, the Raman spectra of a series of 0.5–5% CrO_3/Al_2O_3 samples after calcination at 500°C and re-exposure to the atmosphere were presented and discussed [20]. The 0.5% CrO_3/Al_2O_3 sample showed Ra-

man bands at *ca.* 880 and *ca.* 350 cm^{-1}, which were assigned to the symmetric stretching and bending modes of hydrated surface chromate species (CrO_4^{2-}), respectively [22]. Increasing the surface coverage to 5% CrO_3 resulted in an upward shift of these two modes to 896 and 362 cm^{-1}, respectively, and in the appearance of a new band at 217 cm^{-1}, indicative of Cr–O–Cr linkages. These bands were assigned to hydrated dichromate species ($Cr_2O_7^{2-}$) with 896 cm^{-1}, $\nu_s(CrO_3)$; 362 cm^{-1}, $\delta(CrO_3)$ and 217 cm^{-1}, $\delta(CrOCr)$ [22]. The Raman spectra of supported chromium oxide catalysts possessing moderate and high loadings (5–24% CrO_3/Al_2O_3) are presented in Fig. 1. The Raman spectrum of the 9% CrO_3/Al_2O_3 sample reveals the same bands as the 5% CrO_3/Al_2O_3 sample (also included in Fig. 1) and these bands are accordingly assigned to hydrated dichromate surface species. A small amount of the chromium oxide species is partly dehydrated by the heat of the laser, as indicated by the shoulder on the high frequency side of the strong 896 cm^{-1} band [19–21]. The concentration of the latter species increases in the 12–24% CrO_3 coverage range, as demonstrated by the presence of a pronounced band at *ca.* 1000 cm^{-1} in the corre-

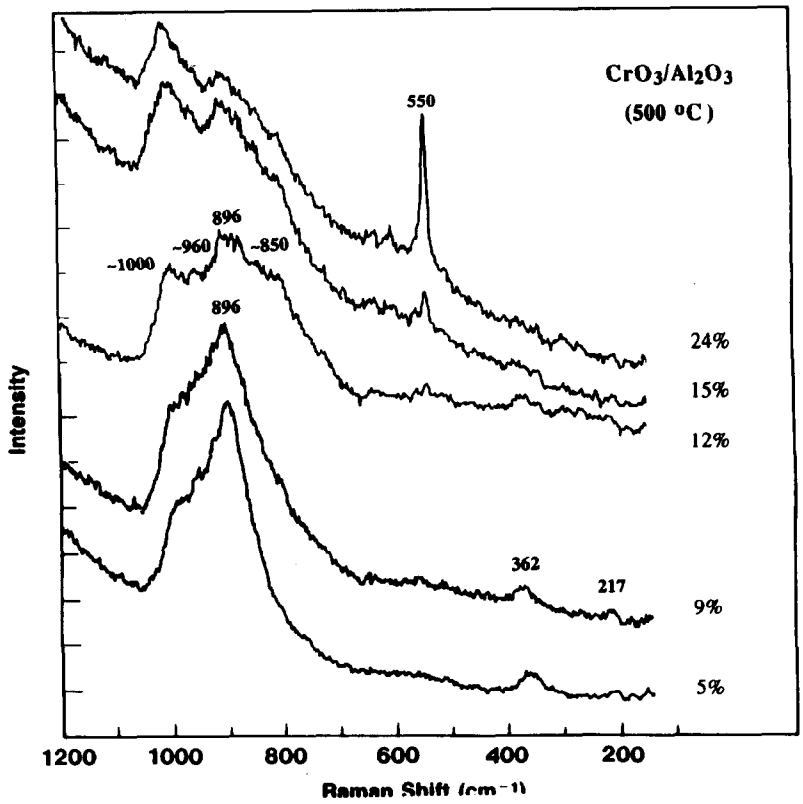

Fig. 1. Raman spectra of CrO_3/Al_2O_3 (calcined at 500 °C) under ambient conditions as a function of the CrO_3 loading.

sponding spectra. This increase is due to darkening of the supported chromium oxide samples with increasing surface coverage (5% CrO_3/Al_2O_3, light yellow to 24% CrO_3/Al_2O_3, brown), which results in an enhanced absorbance of the laser light. The surface structures of the completely dehydrated chromium oxide species after *in situ* thermal treatment have been discussed in a previous article [21]. The spectra of the 12–24% CrO_3/Al_2O_3 samples further show shoulders on either side of the strong 896 cm^{-1} band at *ca.* 960 and *ca.* 850 cm^{-1}, which are indicative of the presence of hydrated trichromate species ($Cr_3O_{10}^{2-}$) on the alumina surface [23]. The *ca.* 960, 896, and *ca.* 850 cm^{-1} bands are accordingly assigned to $\nu_s(CrO_2)$, $\nu_s(CrO_3)$, and $\nu_s(OCrO)$, respectively [23].

The Raman spectra of the 12–24% CrO_3/Al_2O_3 samples further show a sharp band at 550 cm^{-1}, which becomes more pronounced with increasing coverage. This band belongs to metal–oxygen vibration of distorted octahedrally coordinated chromium atoms in crystalline Cr_2O_3 [24]. Thus, the Raman spectra demonstrate that up to a loading of *ca.* 9% CrO_3 the surface chromium oxide species are stabilized in the +6 oxidation state by the alumina support, while at 12% CrO_3, above monolayer coverage, part of the chromium oxide is reduced to the +3 oxidation state forming crystalline Cr_2O_3.

This is further supported by the XPS and XRD measurements. The binding energies of the Cr $2p_{3/2}$ peak of several reference chromium compounds, and of the 5% and 9% CrO_3/Al_2O_3 sample are summarized in Table 1. The binding energies of the two CrO_3/Al_2O_3 samples correspond to chromium oxide in the +6 oxidation state, which is in agreement with a XPS study of Okamoto *et al.* [7]. The X-ray diffraction analysis reveals the presence of Cr_2O_3 crystallites at a surface coverage of 14% CrO_3 and higher after calcination at 500°C, as shown in Table 2. The discrepancy between the Raman and XRD data (12% and 14% CrO_3/Al_2O_3, respectively) for detection of Cr_2O_3 is due to the fact that crystals must be larger than 40 Å to be detected by XRD, while Raman spectroscopy has excellent sensitivity to metal oxide crystallites. A recent infrared spectroscopy investigation of the hydroxyl region and of surface chemisorbed CO_2 species for this CrO_3/Al_2O_3 system showed that most of the OH_{Al}

TABLE 1

Binding energy of Cr $2p_{3/2}$ for chromium compounds and CrO_3/Al_2O_3 catalysts.

Sample	Binding energy (eV) Cr $2p_{3/2}$	Cr valence
Cr	574.1	0
Cr_2O_3	576.6	+3
CrO_3	578.2	+6
5% CrO_3/Al_2O_3 (500°C)	578.4	+6
9% CrO_3/Al_2O_3 (500°C)	578.1	+6

TABLE 2

Influence of surface coverage and calcination temperature on surface area and state of CrO_3/Al_2O_3 catalysts.

Sample	Calcination temperature* (°C)	BET (m^2/g)	XRD phases
γ-Al_2O_3	500	180	γ-Al_2O_3
γ-Al_2O_3	950	94	θ,δ-Al_2O_3
5% CrO_3/Al_2O_3	500	180	γ-Al_2O_3
5% CrO_3/Al_2O_3	950	103	γ-Al_2O_3; θ,δ-Al_2O_3
9% CrO_3/Al_2O_3	500	155	γ-Al_2O_3
12% CrO_3/Al_2O_3	500	160	γ-Al_2O_3
15% CrO_3/Al_2O_3	500	150	γ-Al_2O_3; Cr_2O_3
24% CrO_3/Al_2O_3	500	n.d.[b]	γ-Al_2O_3; Cr_2O_3
24% CrO_3/Al_2O_3	800	n.d.[b]	γ-Al_2O_3; Cr_2O_3; α-Al_2O_3
24% CrO_3/Al_2O_3	950	n.d.[b]	α-Al_2O_3

[a] Calcined for 16 h.
[b] n.d. = not determined.

TABLE 3

Influence of surface coverage on the point of zero surface charge (PZC) of CrO_3/Al_2O_3.

Sample	Calcination temperature (°C)	pH at PZC
γ-Al_2O_3	500	7.8
0.5% CrO_3/Al_2O_3	500	7.3
5% CrO_3/Al_2O_3	500	4.8
9% CrO_3/Al_2O_3	500	3.9
12% CrO_3/Al_2O_3	500	3.7

groups were consumed and that the bands of surface chemisorbed CO_2 species are almost completely suppressed at a surface coverage of *ca.* 12% CrO_3 [25]. This further supports the conclusion that monolayer coverage has been reached at *ca.* 12% CrO_3/Al_2O_3.

The BET surface areas of the supported chromium oxide samples as a function of the loading are also shown in Table 2. These results reveal that the high surface area of the alumina support is maintained after addition of chromium oxide and calcination at 500°C. At higher surface coverages, the catalysts possess slightly smaller surface areas because of the increased catalyst weight due to the addition of chromium oxide.

The PZC for some of the CrO_3/Al_2O_3 samples are shown in Table 3. Alumina itself possesses a pH at PZC of 7.7, while upon introducing chromium oxide the PZC values decrease with increasing surface coverage.

It is well known that in aqueous solutions of CrO_3 different chromium

oxide species are present depending on the chromium concentration and solution pH [22,23]. At low chromium concentrations and under basic conditions, CrO_4^{2-} ions dominate, while in acid solutions at higher chromium concentrations, $Cr_2O_7^{2-}$ ions are present. Under extreme conditions of acidity and high chromium concentration, $Cr_3O_{10}^{2-}$, and probably $Cr_4O_{13}^{2-}$ ions are formed. The following successive equilibria have been proposed for the behaviour of Cr(VI) under varying acidic conditions in aqueous solutions:

$$2CrO_4^{2-} + 2H^+ \rightleftharpoons Cr_2O_7^{2-} + H_2O \quad (1)$$

$$3Cr_2O_7^{2-} + 2H^+ \rightleftharpoons 2Cr_3O_{10}^{2-} + H_2O \quad \text{pH increasing} \quad (2)$$

$$4Cr_3O_{10}^{2-} + 2H^+ \rightleftharpoons 3Cr_4O_{13}^{2-} + H_2O \quad (3)$$

The present Raman spectra of the catalysts also reveal the presence of hydrated chromate, dichromate, and trichromate species, respectively, with increasing loading or decreasing pH at PZC. This similarity exists since after re-exposure to the atmosphere (ambient conditions) the surface of the oxide support becomes hydrated and the surface chromium oxide overlayer is essentially in an aqueous medium. Recently, Deo and Wachs developed a model, based upon this similarity, which predicts the molecular structures of supported metal oxides (such as vanadium, tungsten, molybdenum, and rhenium) under ambient conditions [26]. It was found that the metal oxide surface structures are dependent on the net pH at which the surface possesses zero surface charge. The net surface pH at point of zero charge is determined by the specific support (titania, alumina, silica, etc.) and the surface coverage of the metal oxide. The addition of surface chromium oxide to alumina decreases the pH at PZC of the hydrated surface (see Table 3), and the decrease is proportional to the surface chromium oxide coverage. Consequently, the hydrated chromium oxide structure changes from chromate to dichromate, trichromate, and tetrachromate, and this is similar to the change in structure in aqueous solution as a function of the pH. Recently, exactly the same relationship between structure and PZC has been found for molybdenum and tungsten oxides supported on alumina [27].

Influence of calcination temperature

First the influence of calcination temperature on the γ-Al_2O_3 support has been studied and the resulting Raman spectra are presented in Fig. 2. The Raman spectrum of γ-Al_2O_3 (500°C) is not shown because the γ-Al_2O_3 phase is Raman inactive. Calcination of the alumina support at 950°C transforms the γ-Al_2O_3 phase into a mixture of θ- and δ-Al_2O_3 (major Raman bands at 843, *ca.* 750, and 254 cm^{-1}). The transformation to θ- and δ-Al_2O_3 is confirmed by the XRD analysis, while the BET surface area decreases to 94 m^2/g, as revealed in Table 2. Further calcination at elevated temperatures (1200°C) transforms the alumina to α-Al_2O_3 (major Raman bands at 742, 631, 577, 416, and 378 cm^{-1}). Figure 2 also shows the Raman spectrum of a reference com-

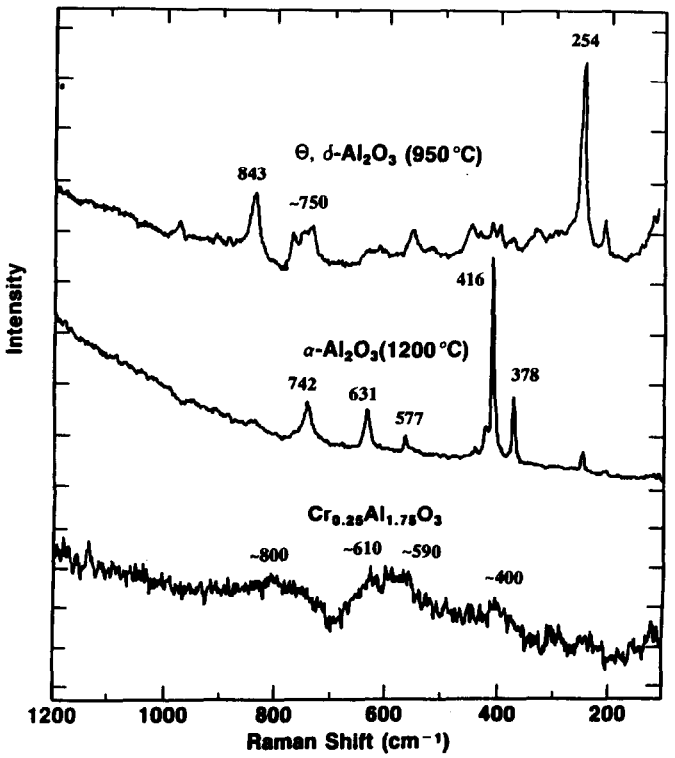

Fig. 2. Raman spectra of $Cr_{0.25}Al_{1.75}O_3$, α-Al_2O_3, and θ,δ-Al_2O_3.

pound, $Cr_{0.25}Al_{1.75}O_3$, which contains Cr(III) in solid solution with α-Al_2O_3(corundum) [20]. This compound exhibits weak and broad Raman bands *ca.* 800, *ca.* 750, *ca.* 610, *ca.* 590, and *ca.* 400 cm^{-1}.

The influence of calcination temperature upon the supported chromium oxide system was studied for the 5% CrO_3/Al_2O_3 (120–1050°C) and 24% CrO_3/Al_2O_3 (500–950°C) sample. Figure 3 shows the Raman spectra of 5% CrO_3/Al_2O_3 as a function of calcination temperature after re-exposure to the atmosphere for 1 h. As described in the experimental section, the supported chromium oxide samples are prepared from aqueous solutions of chromium nitrate. After drying at 120°C, the nitrate is still present, as revealed by the strong $\nu_s(NO_3)$ band at 1050 cm^{-1} [28]. The surface chromium oxide possesses a hydrated chromate structure, CrO_4^{2-}, as demonstrated by the Raman bands at 856 and *ca.* 350 cm^{-1} (very weak) [22]. Thus, drying at 120°C oxidizes the chromium cation from +3 to +6. At first sight, the fact that drying at 120°C oxidizes the chromium cation from +3 to +6 sounds improbable, but support can be found in an article by Fouad *et al.* [29]. Accordingly, the oxidation is initiated near 200°C by topochemical reactions involving atmospheric oxygen

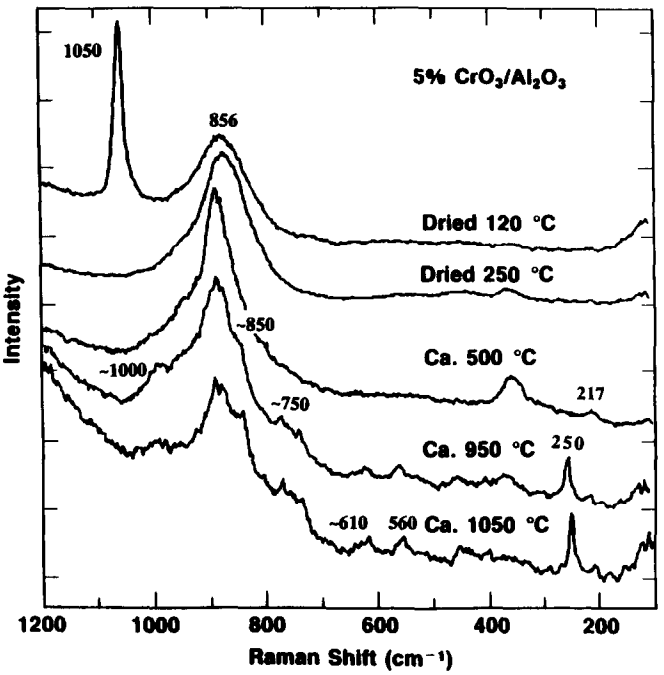

Fig. 3. Raman spectra of 5% CrO_3/Al_2O_3 under ambient conditions as a function of the calcination temperature.

and it proceeds at even lower temperatures in the presence of an active oxidant such as NO_3^-. The nitrate is not stable at higher temperatures as revealed by the complete absence of the strong 1050 cm^{-1} band after drying at 250°C, while the chromium oxide bands are the same as after drying at 120°C and match those of hydrated chromate species. The Raman spectrum recorded after calcination at 500°C has been discussed above and reveals the presence of hydrated dichromate species. After calcination at 950 and 1050°C, the color of the 5% CrO_3/Al_2O_3 sample changed from light yellow (120–500°C) to orange (950–1050°C). This slight darkening of the sample results in some laser-induced dehydration as indicated by a weak band at *ca.* 1000 cm^{-1}. The presence of shoulders at both sites of the strong *ca.* 900 cm^{-1} band at *ca.* 950 and *ca.* 850 cm^{-1} indicates the presence of hydrated trichromate species as discussed above. The Raman spectra further show additional bands after calcination at 950 or 1050°C at *ca.* 750, *ca.* 610, 560, and 250 cm^{-1} due to the formation of θ,δ-Al_2O_3 (see Fig. 2). The transformation of γ-Al_2O_3 to θ,δ-Al_2O_3 at elevated calcination temperatures is also reflected in the XRD patterns and in the dramatic decrease of the BET surface area, as revealed in Table 2. Thus, the alumina support appears to stabilize the +6 oxidation state of the surface chromium oxide up to very high calcination temperatures.

The molecular structure of the surface chromium(VI) oxide species

changes, however, from hydrated chromate, *via* dichromate, to trichromate with increasing calcination temperature. The loading of all samples is the same, 5% CrO_3/Al_2O_3, but the amount of water present on the alumina surface after re-exposure to the atmosphere for approximately 1 h is larger after drying at low temperatures ($\leqslant 250°C$) than after calcination at 500°C [30]. This is because after drying at 250°C the surface is completely dehydrated but after calcination at 500°C also dehydroxylated. The rehydroxylation and water adsorption is probably not completed after 1 h for the sample calcined at 500°C and, therefore, this sample contains less water. Considering equilibria (1), (2), and (3), it is evident that the H_2O content also influences these equilibria. If the water content is lower, as in the case of the sample calcined at 500°C, equilibrium (1) shifts to the right, leading to the formation of dichromate species. Consequently, the net pH of the aqueous film will also be lower after calcination at 500°C than after drying at 250°C. The presence of hydrated trichromate species after calcination at 950 and 1050°C is probably caused by two factors. First, the water content will even be lower than in the case of the sample calcined at 500°C, due to severe dehydroxylation. Second, the significant loss in surface area of the alumina support serves to increase the surface density of the chromium oxide overlayer. The decrease of water content and increase of surface density results in a shift of equilibrium (2) to the right leading to a further reduction of the net pH at PZC of the hydrated oxide surface and formation of trichromate species.

The Raman spectra of the 24% CrO_3/Al_2O_3 sample under ambient conditions after calcination at different temperatures are presented in Fig. 4. The Raman spectrum obtained after calcination at 500°C has been discussed above and it was shown that in addition to some laser-induced dehydrated chromium oxide species and hydrated trichromate species, crystalline Cr_2O_3 particles are present on the alumina surface. After calcination at high temperatures ($\geqslant 800°C$), the Cr_2O_3 particles are not stable since the 550 cm^{-1} band decreases in intensity and is completely absent after calcination at 950°C. The Raman spectrum after calcination at 950°C further shows bands at *ca.* 800, *ca.* 750, *ca.* 610, *ca.* 590, and *ca.* 400 cm^{-1}, which match those of $Cr_{0.25}Al_{1.75}O_3$ (see Fig. 2). The XRD analysis of the 24% CrO_3/Al_2O_3 sample also reveals that the amount of Cr_2O_3 decreases after calcination at 800°C and that α-Al_2O_3 is formed (Table 2). The α-Al_2O_3 phase formed from the 24% CrO_3/Al_2O_3 at high calcination temperatures, however, possesses lattice parameters slightly different from those of an α-Al_2O_3 reference sample as shown in Table 4. Both parameters a and c appear to be slightly larger than for crystalline α-Al_2O_3. Thus, the Raman spectra and XRD data reveal that at higher calcination temperatures crystalline Cr_2O_3 reacts with alumina to form a solid solution of Cr^{3+} in α-Al_2O_3. A similar observation has been made by Saleh *et al.* for a 7% V_2O_5/TiO_2 sample after calcination at elevated temperatures [31]. The disappearance of the Raman band of crystalline V_2O_5 and the distortion of the titania (rutile) lattice was attributed to the formation of a substitutional solid solution of V^{4+} in TiO_2 (rutile), $V_xTi_{1-x}O_2$.

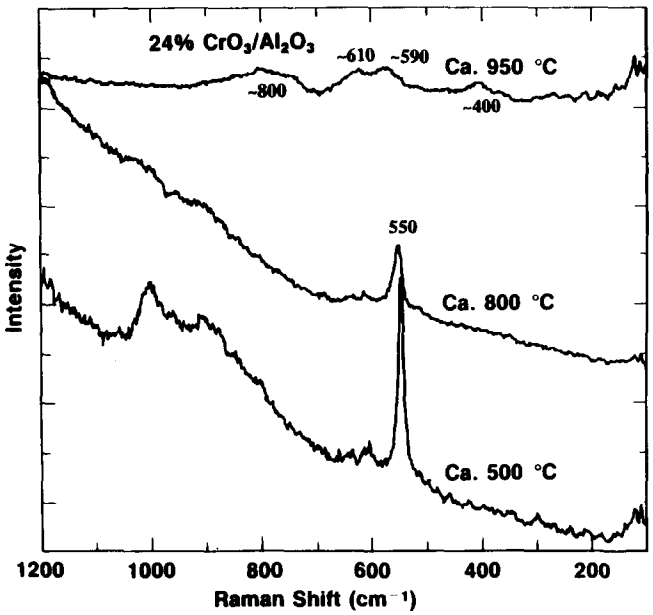

Fig. 4. Raman spectra of 24% CrO_3/Al_2O_3 under ambient conditions as a function of the calcination temperature.

TABLE 4

Lattice parameters of α-Al_2O_3 phase formed from CrO_3/Al_2O_3 at high calcination temperatures.

Sample	a (Å)	c (Å)
α-Al_2O_3	4.7616(8)	12.995(4)
24% CrO_3/Al_2O_3 (800°C)	4.816(6)	13.10(1)
24% CrO_3/Al_2O_3 (950°C)	4.7906(6)	13.075(3)

Conclusions

It was found that up to a surface coverage of 9% CrO_3/Al_2O_3 chromium oxide is stabilized by the alumina support in the +6 oxidation state after calcination at 120–1050°C. The molecular structures of the hydrated chromium(VI) oxide surface species, however, are a function of the surface coverage and calcination temperature. This is because the surface structures are dependent on the net surface pH at PZC of the hydrated oxide surface. Increasing the surface coverage results in a decrease of net surface pH and formation of more polymerized chromium oxide species (dichromates, and trichromates). High calcination temperatures cause a reduction of the BET surface area and results in an increase of the surface density of the chromium oxide overlayer. The net surface pH decreases by the increase of surface density and,

consequently, more polymerized chromium oxide species (trichromates) are found on the alumina surface. Monolayer coverage is reached at *ca.* 12% CrO_3/Al_2O_3 and crystalline Cr_2O_3 particles are found on the alumina surface together with surface chromium oxide species. At high calcination temperatures ($\geq 800°C$) the Cr_2O_3 crystalline particles react with the alumina support to form Cr(III) in solid solution with α-Al_2O_3(corundum). The α-Al_2O_3 lattice is slightly expanded due to the incorporation of chromia.

Acknowledgements

The authors thank J. Ekerdt and C.R. Narayanan for measuring the surface pH and D.J. Stufkens and A. Oskam for useful discussions.

References

1 C.L. Thomas, Catalytic Processes and Proven Catalysis, Academic Press, New York, 1970.
2 M.P. McDaniel, J. Catal., 76 (1982) 17.
3 C.P. Poole and D.S. MacIver, J. Chem. Phys., 41 (1964) 1500.
4 M. Richter, E. Alsdorf, R. Fricke, K. Jancke and G. Öhlmann, Appl. Catal., 24 (1986) 117.
5 D.D. Beck, J.H. Lunsford, J. Catal., 68 (1981) 121.
6 R. Merryfield, M. McDaniel and G. Parks, J. Catal., 77 (1982) 348.
7 Y. Okamoto, M. Fujii, T. Imanaka and S. Teranishi, Bull. Chem. Soc. Jpn., 49 (1976) 859.
8 A. Cimino, B.A. De Angelis, A. Luchetti and G. Minelli, J. Catal., 45 (1976) 316.
9 A. Zecchina, E. Garrone, G. Ghiotti, C. Morterra and E. Borello, J. Phys. Chem., 79 (1975) 966.
10 A. Ellison and K.S.W. Sing, J. Chem. Soc., Faraday Trans. 1, 74 (1978) 2017.
11 B. Fubini, G. Ghiotti, L. Stradella, E. Garrone and C. Morterra, J. Catal., 66 (1980) 200.
12 M.P. McDaniel, J. Catal., 67 (1981) 71; 76 (1982) 29; 76 (1982) 17; 76 (1982) 37; 77 (1982) 348; 101 (1986) 446.
13 D. Cordischi, V. Indovina and M. Ochiuzzi, J. Chem. Soc. Faraday Trans., 87 (1991) 3443.
14 A. Cimino, D. Cordischi, S. Febraro, D. Gazzoli, V. Indovina, M. Occhiuzzi and M. Valigi, J. Mol. Catal., 55 (1989) 23.
15 A. Cimino, D. Cordisichi, S. De Rossi, G. Ferraris, D. Gazzoli, V. Indovina, G. Minelli, M. Occhiuzzi and M. Valigi, J. Catal., 127 (1991) 744.
16 V. Indovina, D. Cordischi, S. De Rossi, G. Ferraris, G. Ghiotti and A. Chiorino, J. Mol. Catal., 68 (1991) 53.
17 A. Iannibello, S. Marengo, P. Tittarelli, G. Morelli and A. Zecchina, J. Chem. Soc., Faraday Trans. 1, 80 (1984) 2209.
18 M. Richter, P. Reich and G. Öhlmann, J. Mol. Catal., 46 (1988) 79.
19 M.A. Vuurman, D.J. Stufkens, A. Oskam, J.A. Moulijn and F. Kapteijn, J. Mol. Catal., 60 (1990) 83.
20 F.D. Hardcastle and I.E. Wachs, J. Mol. Catal., 46 (1988) 173.
21 M.A. Vuurman, I.E. Wachs, D.J. Stufkens and A. Oskam, J. Mol. Catal. 80 (1993) 209.
22 G. Michel and R. Machiroux, J. Raman Spectrosc., 14 (1983) 22.
23 G. Michel and R. Machiroux, J. Raman Spectrosc., 17 (1986) 79.
24 I.E. Beattie and T.R. Gilson, J. Chem. Soc. A, (1970) 980.
25 A.M. Turek, I.E. Wachs and E. Decanio, J. Phys. Chem., 96 (1992) 5000.

26 G. Deo and I.E. Wachs, J. Phys. Chem., 95 (1991) 5889.
27 S.D. Kohler, J.G. Ekerdt, D.S. Kim, and I.E. Wachs, Catal. Lett., 16 (1992) 231.
28 K. Nakamoto, Infrared Spectra of Inorganic and Coordination Compounds, J. Wiley and Sons, New York, 1963.
29 N.E. Fouad, H. Knözinger, M.I. Zaki and A.A. Mansour, Z. Phys. Chem., 171 (1991) 75.
30 H.-P. Boehnm and H. Knözinger, in J.R. Anderson and M. Boudart, (eds.), Catalysis – Science and Technology, vol. 4, Springer-Verslag, West Berlin, 1983, p. 39.
31 R.Y. Saleh, I.E. Wachs, S.S. Chan and C.C. Chersich, J. Catal., 98 (1986) 102.